Computers and Chemical Engineering 122 (2019) 47–58

Contents lists available at ScienceDirect

Computers and Chemical Engineering

journal homepage: www.elsevier.com/locate/compchemeng

Optimal design of aging systems: A-frame coolers design under fouling

José A. Luceño, Mariano Martín*

Departamento de Ingeniería Química y Textil. Universidad de Salamanca. Pza. Caídos 1-5, Salamanca 37008, Spain

ARTICLE INFO

Article history:
Received 23 January 2018
Revised 27 March 2018
Accepted 16 May 2018
Available online 17 May 2018

Keywords:
Energy
Concentrated solar power
Dry cooling
Mathematical Optimization
Simultaneous unit design and operation

ABSTRACT

This work presents a parametric programming framework for the optimal design and operation of systems with performance loss over time. A two-stage procedure is proposed. The unit is designed for the operating conditions just before maintenance. In a second stage, a multiperiod problem is solved for the optimal the operation of the unit over time including cleaning costs. The minimum operating cost as a function of the cycle length determines the operating cycle and the unit design. The methodology is applied to A-frame cooling systems under fouling conditions, where fouling affects the pressure drop and the global heat transfer coefficient. The sigmoidal deposition profile results in an optimal cycle time of 8 years. This design allows reducing the energy required to around 4% of the energy produced by the concentrated solar power plant. It is a promising result that can be affected by plant layout and ground availability.

1. Introduction

Everyday operation causes fatigue to materials and dirt deposits build on the surface of equipment. As a result, these units suffer losses in performance over time that affect the overall yield of the unit and of the facility. Beyond the lost in performance, failures may occur if the units operate for longer periods. Eventually, some of the units or sections must be replaced or repaired. It is estimated that $20,000–$30,000 of losses per hour can occur in refineries due to failures due to lack of proper maintenance (Tan and Kramer, 1997). Industry schedules maintenance shutdowns to evaluate the status, mitigate risks, clean and repair sections and entire units. In the literature, there is a large number of methods to evaluate maintenance strategies, most of them in the field of chemical and mechanical engineering, but also in logistics, where planes, train, trucks or ships are subjected to regular maintenance (Dekker, 1996). However, the most common optimization is minimum cost subject to average uptime or downtime (Mukerji et al., 1991; Wang, 2002) and mitigation strategies are developed based on the performance decay or the aging process (Kijima and Sumita, 1986; Damaso and García, 2009; Beaurepaire et al., 2012). Different tools have been developed to help schedule maintenance (Nguyen et al., 2008). To the best of our knowledge, simultaneous design and operation of the units considering performance decay is not addressed, although for instance the design of structures considers aging (Dekker, 1996).

Concentrated solar power (CSP) plants are typically located in regions with high solar incidence but limited water availability (Martín and Martín, 2013). For years, water consumption was not an issue in industry. However, it is no longer the case (Rosegrant, 2002). Wet cooling towers have been used and proved efficient, but the consumption of water adds up to around 2 L per kWh produced, a luxury that desert regions cannot afford (Martín and Martín, 2017). The large cooling needs required by any thermal plant using wet cooling systems are responsible for the water-energy nexus involved in power production (DOE, 2018). A large Energy–Water–Food initiative is being put together to address inefficiencies that lead to unsustainable operation of industrial and agricultural systems (FAO, 2018). Lately, several efforts have been carried out to limit the consumption of water using a particular design of air coolers, A-frames. These units are characterized by their pipe configuration in the form of an “A”, and promising cooling efficiencies (Martín, 2015). However, the consumption of up to 10% of the power generated in the facility to operate the fans is an important drawback. The design of such units has typically been carried out based on heuristics (Kröger, 2004; Heyns, 2008) and optimization studies for the design were limited to a small number of variables (Bredell and Kröger, 2006). Recently, Luceño and Martín (2018) developed a detailed mathematical optimization framework for the optimal design and annual operation of an A-frame cooling systems. The work reported promising savings in the operation of these units.

* Corresponding author.
E-mail address: mariano.m3@usal.es (M. Martín).

https://doi.org/10.1016/j.compchemeng.2018.05.015
0098-1354/

Nomenclature

A_{in}	inside total area, m^2
A_{out}	outside total area, m^2
$Amort_{equipment}$	amortization of an equipment, $\$_{2014}$/month
$C_{\$-kWh}$	kWh price, $\$_{2014}$/kWh
C_{elec}	energy cost, $\$_{2014}$/month
$C_{equipment}$	cost of an equipment, $\$_{2014}$
C_{fan}	cost of a fan, $\$_{2014}$
C_{frame}	heat exchanger cost, $\$_{2014}$
$C_{cleaning}$	cost of a cleaning stage, kW
$C_{p_{air}}$	air heat capacity, kJ/(kg K)
$C_{p_{w.vap}}$	water steam heat capacity, kJ/(kg K)
D_f	outer fin diameter, m
d_{ts}	width of support beam, m
$DeLi_{equipment}$	expected life of an equipment, year
f	binary parameter of the fan during the month
f_j	resistance to the heat transfer in side j, (K m^2 s)/ kJ
Fouling	coefficient of the increase in the pressure drop due to fouling
H	humidity of the air, kg/kg
K_2	K_2 term of fan cost
L_t	pipe length, m
L_{ts}	length of support beam, m
$LMTD$	logarithm mean temperature difference, K
m_{air}	air mass flow, kg/s
m_{fan}	air mass flow per fan, kg/s
m_w	water vapor mass flow, kg/s
n_b	number of bundles working corresponding to the studied fan
n_f	number of fins per tube
n_{fan}	number of fans
$n_{cleaning}$	number of cleaning stages
n_{cycles}	number of operating cycles
N_r	number of rows per bundle
N_t	number of pipes per row
P_F	power supplied by a fan on his shaft, kJ/s
P_{vent}	total power supplied by fans, kJ/s
Q	heat flow, kJ/s
Q_{air}	total air volume flow, m^3/s
R	fouling resistance (K m^2 s)/ kJ
$T_{in,\ air}$	inlet air temperature, K
$T_{out,\ air}$	outlet air temperature, K
t	time (years)
U	overall heat transfer coefficient, kJ/(K m^2 s)
V_{air}	air volume flow per fan, m^3/s
v_{std}	air volume flow at standard conditions, m^3/s
x_{do}	downstream obstacles from the fan, m
x_{up}	upstream obstacles from the fan, m

Greek letters

γ_{pt}	fan blade's angle,°
Δp_e	total pressure drop across the system unit, Pa
ΔT_a	temperature difference at the entrance of the heat exchanger, K
ΔT_b	temperature difference at the exit of the heat exchanger, K
λ_w	latent heat of evaporation of the water steam, (kJ/kg)

Subscript

(m)	month
i	ith element of the set
tot	total monthly value of a variable

Superscript

A-frame units are located in open air and fouling, in particular, particle fouling is an important issue for their operation and performance. Fouling phenomena have been long studied for heat exchangers (Kern and Seaton, 1959) and the rate of deposition and fouling have been modelled in the literature (Muller-Steinhagen et al., 1988,2005). Design books present characteristic factors to estimate the effect of fouling on the loss of heat transfer efficiency due to the deposition of dirt on the pipes (Coker, 2007; Walas, 1990; Zammit 2005; GEA, 2008; Towler and Sinnott, 2008). Müller-Steinhagen et al. (2011) stated that conservative designs represent 0.25% of the gross domestic product of industrialized countries and several cleaning strategies were discussed. However, from the design perspective the effect of deposits nature and building-up have not been evaluated until recently. The synthesis of heat exchanger networks under fouling conditions has been addressed at design level by Liu et al. (2015) and at control level by Luo et al. (2013) to mitigate the performance decay. Díaz-Bejarano et al. (2017) developed a systematic approach for the analysis and characterization of fouling and cleaning in refinery heat exchangers. In the case of air coolers, particle deposition is the main issue (Ahn et al., 2006).

When operating A-frames, fouling does not only affect the heat transfer coefficient, but deposits also block the cross sectional area, generating an additional pressure drop across the bundle of pipes (Pu et al., 2009; Sarfraz and Bach, 2016). An experimental example that determined the effect of particle fouling on the global heat transfer coefficient and the pressure drop showed that for single-row heat exchangers, the pressure drop increased by 28–31%, while the heat transfer performance decreased by 7–12% when 300 g of standard dust was sprayed (Pak et al., 2003). Therefore, the share of the power produced by the facility to be devoted to operating the fans increases with time. Several lab scale studies have been developed showing the effect of particle deposition on pressure drop for air coolers (Ahn et al., 2006) as well as that on the heat transfer coefficient (Haghighi-Khoshkhoo and McCluskey, 2007) or considering the effect of fouling on both (Bell et al., 2009).

In this work we present a general methodology for the simultaneous optimal design and operation of units or processes whose yield is affected by aging or performance decays. In this case aging refers to the loss of efficiency due to fouling. We propose a parametric programming design procedure to determine the design and the cleaning/maintenance schedule. We use it for the design of A-frames under fouling conditions. We extend the previous model of an A-frame developed by Luceño and Martín (2018) to account for the effect of fouling on both, the heat transfer resistance and the pressure drop. The paper is organized as follows: In Section 2, the methodology is described. In Section 3 the modelling features of the case of study are presented focusing on the effect of particle fouling on the pressure drop across the pipe bundle and on the heat transfer coefficient. Next, in Section 4 the case study and the main results are discussed such as design features comparing the clean and the dirty designs, and major operating conditions including the power consumed by the cooling system, as well as the usage of area and number of fans. Finally, Section 5 draws some conclusions.

2. Unit design and operation under aging

This methodology is generic for any phenomenon that decreases the yield or performance of a unit or a process over time. It is based on a parametric optimization approach for the simulta-

neous design and operation of the unit. The parameter is the cycle time, the years of operation before a maintenance shutdown. First, a detail model of the unit or facility is to be developed. Special attention is to be paid to identify the performance/yield variables. Next, the yield decay must be characterized and its effect on the operating variables must be modelled. Before applying the methodology, the lifetime of the plant is to be estimated to determine the operating horizon.

The methodology consists of two stages. The length of the operating cycle is an optimization parameter. For a fixed cycle time period before maintenance, the unit is designed to operate under the worst conditions, those corresponding to just before cleaning, a robust design. The variables affected by aging are estimated from the decay laws under these conditions. Then, the design of the unit is optimized by solving the detail mathematical model using the operating costs, OPEX, as objective function.

For the fixed design determined by a particular length cycle, we formulate a multiperiod optimization problem. The variables affected by aging are computed beforehand using the decay laws. The time step is variable depending on the operating horizon. The objective function is the OPEX over the entire operating period. Cleaning steps may have a cost. It can be estimated as the profit that is not obtained during the cleaning stage assuming the production capacity of the month/months before cleaning, depending on the performance of the plant, or it can be fixed. The cleaning or maintenance costs are added to the objective function for as many stops as needed along the entire lifetime of the unit. If there is not an integer number of operating periods to cover the entire lifetime, a fraction is added and so its cost, to the OPEX for comparison among cleaning schedules.

A different operating horizon is fixed, and the procedure is repeated until the OPEX does not longer decreases. Therefore, the worst case is optimized.

By solving this two-stage problem for different operating horizons, the optimal operating horizon before cleaning is computed so that both the maintenance schedule and unit design are simultaneously addressed. Fig. 1 shows a generic scheme of the procedure. In dashed lines the data computed for the particular example described below, that can be substituted by the operating variables subjected by aging in the particular case.

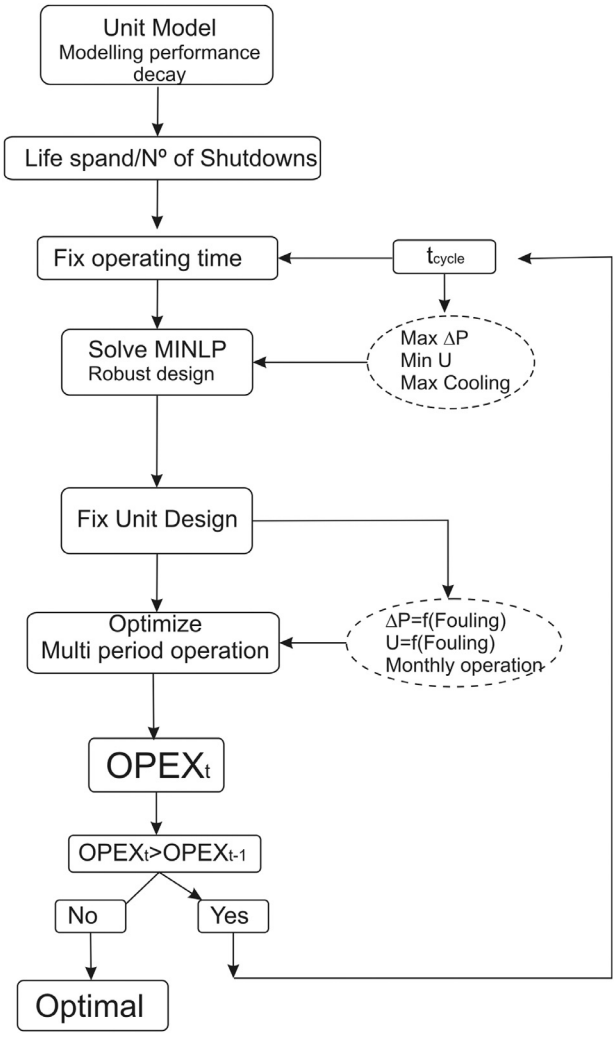

Fig. 1. Scheme of the algorithm.

3. Case of study

We consider the case of the optimal design of A-frame systems under fouling conditions within the operation of CSP plants. These units are located in the open air, and therefore subjected to weather conditions. In particular, deposits build on the heat exchanger pipes affecting both the pressure drop and the heat transfer coefficient. Thus, the aging variables are the global heat transfer coefficient and the pressure drop.

3.1. CSP facility description

The plant consists of three sections: the heliostat field, including the collector and the molten salts storage tanks, the steam turbine and the air cooler steam condenser. Fig. 1S in the supplementary material presents the flowsheet for the process. This process is based on the use of a tower to collect the solar energy and a regenerative Rankine cycle. The steam is generated in a system of three heat exchangers where water is heated up to saturation and then evaporated using the total flow of molten salts. However, only a fraction of the flow of salts is used to superheat the steam before it is fed to the first body of the turbine. The rest is used to reheat up the steam before it is fed to the medium pressure turbine. In the medium pressure turbine, part of the steam is extracted and it is used to heat up the condensate. The rest of the steam is finally expanded to an exhaust pressure, condensed and recycled. For the condensation of the steam we propose the use of a direct air cooler system, an A-frame. For the detailed information on the modelling features of the heliostat field and the steam turbine, we refer to previous work (Martín and Martín, 2013; Martín, 2015).

3.2. Air cooling system

The exhaust steam from the turbine circulates along a large pipe and it is distributed into the inclined pipes that form a roof over a system of fans in the form of an A. The steam is condensed in the tubes as it descends. Fig. 2S shows a scheme of a typical A-frame condenser.

3.3. A-frame model structure

The model extends previous work to include the effect of fouling on the heat transfer coefficient and on the pressure drop. Thus, the model is divided in 3 sections: mass and energy balances, A-frame design, and fans design. For the sake of the length of the paper we focus on modelling the effect of fouling on the global heat transfer coefficient and the pressure drop. The details of the geometry of the A-frame can be found in the supplementary material as well as in previous work (Luceño and Martín, 2018).

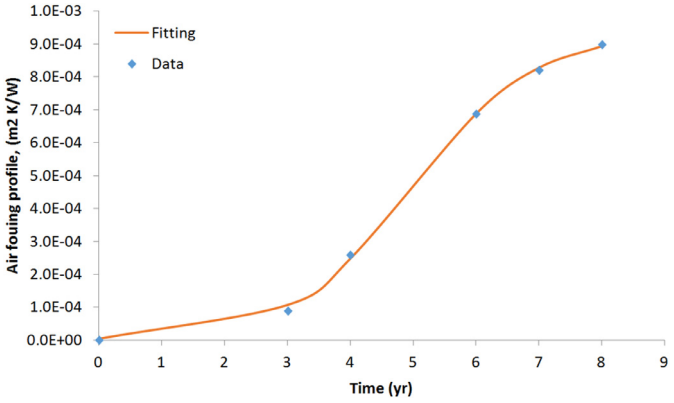

Fig. 2. Fouling resistance of in the air side over time.

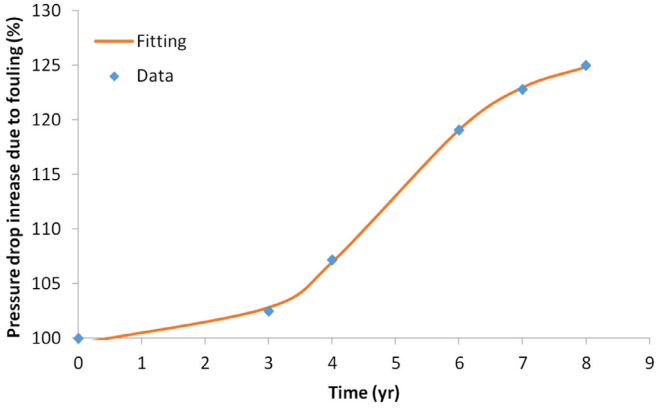

Fig. 3. Pressure drop increase over time under fouling conditions.

3.3.1. Mass and energy balances

Two energy balances are formulated, one for the air flow and another one for the steam. The first one determines the air flow required for the operation, and is given by Eq. (1):

$$Q = m_{air} \cdot \left[C_{p_{air}} \cdot (T_{out,air} - T_{in,air}) + H \cdot C_{p_{w,vap}} \cdot (T_{out,air} - T_{in,air})\right] \quad (1)$$

The energy that has to be rejected, Q, is computed from the energy balance to the steam, as given by Eq. (2) and the data of the operation of the CSP plant (Martín and Martín, 2013).

$$Q = m_w \cdot \lambda_w \quad (2)$$

3.3.2. A-frame design

The general design equation of any heat exchanger is Eq. (3):

$$Q = U \cdot A_{out} \cdot LMTD \quad (3)$$

LMTD is computed using Chen's approximation (Chen, 1987). A_{out} is that given by finned pipes. The total are, A_{out}, is computed by the number of pipes per row and bundle and the fines that they have, see supplementary material.

The global heat transfer coefficient, U, is affected by fouling. Therefore, we need to correct it as follows:

$$\frac{1}{U} = f_{air} + R_{air} + f_{tube} + f_{steam} + R_{steam} \quad (4)$$

The terms related to the air and steam sides, f_{air}, f_{steam}, and that of the tube, f_{tube}, remain the same as previous work (Luceño and Martín, 2018). However, to account for fouling we assume that the resistance to the air side as a function of time increases. There are a number of typical trends depending on the type of deposit from linear (Al-Haj Ibrahim, 2012) to logarithmic based. Typically, the thickness of a deposit is a measure of the resistance of the deposit to the transfer of heat. Therefore, based on the results for particle deposition in air coolers by Ahn et al. (2006), we assume that the resistance to heat transfer due to fouling follows the same profile as that of the pressure drop. We use values from tables in design books for the actual final value and, according to the profile for deposition (Ahn et al., 2006; Yang et al 2007; The Engineering Toolbox, 2018), it is assumed that the resistance to fouling is reached after 8 years. Fig. 2 shows the increase in the fouling resistance to heat transfer over time. Eq. (5) presents the fitting correlation. The increase in the resistance due to fouling on the steam side, Eq. (6), is assumed to be linear with time.

$$R_{air} \cdot 10^4 = \frac{9.379}{1 + e^{5.091 - 1.020 \cdot t}} - 2.400 \times 10^{-2} \quad (5)$$

$$R_{ws} = 1.1250 \times 10^{-5} \cdot t(years) \quad (6)$$

3.3.3. Fans design

The deposition of dust on the pipes increases the pressure drop across the pipe bundle. As a result, the energy consumption increases so as to be able to move the air flow to condense the exhaust steam. In this model we use the same blade designs as in a previous work (Luceño and Martín, 2018).

3.3.3.1. Power per fan. The power required by the fan is that needed to overcome the pressure drop, and can be obtained from Eq. (7):

$$P_{vent} = n_{fan} \cdot P_F = Q_{air} \cdot \Delta p_e \quad (7)$$

where P_F is given by Luceño and Martín (2018)

$$P_F = \left(1.3122 \times 10^{-5} \cdot \gamma_{pt} - 6.7710 \times 10^{-4}\right) \cdot V_{air}^2 + \left(1.4015 \times 10^{-2} \cdot \gamma_{pt} + 4.1596 \times 10^{-1}\right) \cdot V_{air} \quad (8)$$

The number of fans is computed as follows, Eq. 9:

$$Q_{air} = n_{fan} \cdot V_{air} \quad (9)$$

3.3.3.2. Pressure drop . The pressure drop across the system is the one responsible for the energy consumed by the fans. To compute it, we need to account for the different contributions such as the pressure drop at the entrance of the structure, f_s, before, f_{bfans}, and after the fan, f_{afans}, and finally across the tubes bundles, f_{bundle}, apart from the pressure drop across the fan itself, Δp_{Fs} see Eq. (10). The details of each one of the terms can be seen in the supplementary material or in previous work (Luceño and Martín, 2018). However, fouling modifies the pressure drop across the pipes bundle.

$$\Delta p_e = -\left[f_f + f_{bfans} - \Delta p_{Fs} + f_{afans} + f_{bundle} \cdot Fouling\right] \quad (10)$$

In order to compute the increase in the pressure drop generated in the bundles of tubes over time, experimental data from the literature have been used. Bell (2007) shows experimental data for three levels of fouling for different velocities. Based on those values, we see that the effect of velocity on the contribution of fouling to pressure drop is already considered within the clean model. Kern and Seaton (1959) proved that there is an asymptotic thickness of the fouling layer. It is expected that pressure drop will follow the same trend. Using the experimental data from Ahn et al. (2006), it is possible to fit the increase in the pressure drop as a result of particle fouling over time. Fig. 3 shows the profile of the increase in the pressure drop due to fouling. Rhombus represent the experimental dada and the line plots the model given by Eq. (11).

$$Fouling = 0.01\left(\frac{26.891}{1 + e^{4.806 + 0.973 \cdot t(years)}} + 126.172\right) \quad (11)$$

3.4. Design of A-frames under fouling conditions

To determine the optimal design and cleaning scheme a parametric optimization framework is proposed, see Fig. 1. The parameter is the number of years before cleaning, always above 3 years and typically below half-life of the unit, 8 years. In general, the cycle time could be extended up to the lifetime. However, we assumed at least one maintenance shutdown and the fact that by the time the unit is decommissioned it should to be left clean. Thus, from 8 years to a maximum of 13 years would have been possible, based on the fact that for 3 years fouling does not present performance decays. The algorithm works as follows. For the maximum dirty conditions, by the end of the cycle, we design the unit for the month of the maximum cooling load. We solve an MINLP using a Taylor made Branch and Bound algorithm to determine the number of bundles, pipes, fans and the geometry of the unit.

The accumulation of dust reduces U and increases the pressure drop as presented in the model above. Over the horizon period before the next maintenance shutdown for cleaning we optimize the operation and determine the costs. With the geometrical design already fixed, we compute U clean for the different months along that final year of operation. Each of them is used as reference to compute the clean ones of the corresponding months of the first year of operation by removing the contribution of the fouling. With the clean U, we finally recompute U for all other months of the operating period. We also compute a coefficient, the increase of the pressure drop on a monthly basis using Eq. (11). We assume that the solar profile will be similar over the years, but that can be updated using prediction algorithms i.e. ARIMA. We solve the MINLP for the number of months corresponding with the operation before cleaning. Multiperiod optimization is required. If the problem becomes large, a rolling horizon scheme can be implemented. The solution to this problem provides an operating cost for this period. We compute the number of cleaning stages and provide a cost for cleaning. Several costs are considered, including no cleaning costs and three different costs. The cleaning costs considered correspond to the production capacity of one month of operation. That does not mean that it takes one entire month for maintenance. We use the monthly maximum, minimum and average production capacities over a year to evaluate the effect of cleaning costs on the solution performing a sensitivity analysis. Finally, since the life time of the unit is assumed to be 16 years (MPR, 2014), there is an additional cost for the additional years until the unit is to be decommissioned as a fraction of the operating cost of the entire period computed by the MINLP problem.

3.4.1. Optimal equipment design

The objective function is based on the annualized cost of the unit including the cost of operation. The estimation of the cost of the units is based on the equipment cost to compute the facility investment cost, and the power consumed to run it, as the operating cost. The equipment cost can be divided into fan cost and A-frame heat exchanger cost. The equipment cost can be estimated using Eqs. (12)–(14) (Manassaldi et al., 2014; Matche 2014):

$$C_{frame} = 3109 \cdot A^{0.40} \tag{12}$$

$$C_{fan} = K_2 \cdot 2.2 \cdot [1 + 0.2164 \cdot \ln(\Delta p_e)] \tag{13}$$

$$K_2 = 10^{2.9471 + 0.3302 \cdot \log_{10}(v_{std}) + 0.1969 \cdot \log_{10}(v_{std})^2} \tag{14}$$

The monthly amortization, Eq. (15), is determined considering that the expected life of the A-frame bundles and the fans, both assumed to be 16 years (MPR, 2014):

$$Amort_{equipment} = \frac{C_{equipment}}{12 \cdot DeLi_{equipment}} \tag{15}$$

The cost for the power consumed is estimated using Eq. (16):

$$C_{elec} = \frac{1}{\eta_{fan}} \cdot P_F \cdot \left(744 \frac{kWh \cdot s}{kJ \cdot month}\right) \cdot C_{\$-kWh} \tag{16}$$

Finally, cleaning cost is added and is multiplied by the number of cleaning instances over the lifespan on the unit. Thus, the objective function becomes, Eq. (17):

$$Z = Amort_{frame} + Amort_{fan} + C_{elec} + n_{ckeaning} \cdot C_{cleaning} \tag{17}$$

Subject to the model is described in Section 3.3. See supplementary material for further details.

A Taylor made Branch and Bound method is used to solve the MINLP based on a deep first approach. We start by branching on the number of rows N_r, next the number of tubes per row N_t, subsequently the number of bundles of tubes,N_b. At this point we use the D_f as lower bound for X_t andX_l. The next level of the tree corresponds to the inner diameter and the outer diameter of the tubes D_{in} and D_{out}. Subsequently, the tube length L_t is fixed using intervals of 0.15 m (Wallas, 1990). At this point we already fix the number of fins per tube length, n_f, and the fins diameter D_f. Finally, the number of fans n_{fan} is computed. Each relaxed NLP problem at any node corresponds to a highly nonlinear, non convex model of about 150 eqs. and variables. It is solved using a multi-start initialization procedure using CONOPT as preferred solver.

3.4.2. Optimal operating conditions

The optimal geometric design provided by the previous problem is applied to evaluate the unit operating conditions on a monthly basis. The monthly operating conditions are determined by solving a multi-period optimization model. The objective function is the minimization of the energy consumption. However, for such a model to be solved, the highly non-linear equations of the design model must be simplified. First, all variables related to the mechanical design of the equipment (pipes, bundles, fans and support structure's specifications) are fixed using the results of the optimal design. Then, the coefficients that depend on the geometry are also computed and fixed. Air thermodynamic properties are also fixed to average annual values since there is not much variation throughout the year.

Next, the variables are transformed into monthly depended parameters or variables. In particular, the fouling coefficient to compute the pressure drop and the global heat transfer coefficient as described above. Fig. 5 shows the values of U that have been included in the formulation. Similarly, using the deposit growing rate, we compute the profile of increase in the pressure drop as a function of time, see Fig. 6.

Finally, we also have: $A_{out}(m)$, $Q(m)$, $LMTD(m)$, $\Delta T_a(m)$, $\Delta T_b(m)$, $T_{out,\ air}(m)$, $T_{in,\ air}(m)$, $m_{air}(m)$, $m_w(m)$ and $Q_{air}(m)$. These variables cannot be fixed because the area used or needed, the air flow and the energy balances change on a monthly basis.

Thus, the multi-period model involves the energy balances, the design equation for the heat exchanger and a set of equations grouped into four blocks as follows:

–Global equations: the Eqs. (18) and (19):

$$n_b^{tot}(m) = \sum_{i=1}^{n_{fan}} n_b^i(m) \tag{18}$$

$$Q_{air}(m) = \sum_{i=1}^{n_{fan}} V_{air}^i(m) \tag{19}$$

–Fan's equations: the Eqs. (20)–(23):

$$V_{air}^i(m) \le f^i(m) \cdot 700 \tag{20}$$

$$V_{air}^i(m) \ge f^i(m) \cdot 50 \tag{21}$$

Table 1
Atmospheric conditions (Martín and Martín, 2013).

Month	kWh/m^2·day	Day	SUN (H)	Sun(h/day)	$T_{in,\ air}$ (°C)	% Humidity
January	4.377	31	191	6.161	12.5	69
February	5.125	28	191	6.821	13.2	68
March	5.319	31	228	7.355	14.7	66
April	6.387	30	250	8.333	16.4	64
May	6.697	31	299	9.645	19.1	66
June	8.587	30	322	10.733	22.7	64
July	8.668	31	338	10.903	25.7	63
August	7.342	31	312	10.065	26.4	65
September	6.057	30	257	8.567	24.0	66
October	4.126	31	221	7.129	20.0	68
November	3.513	30	187	6.233	16.2	70
December	3.326	31	176	5.677	13.7	70
Average	5.794	30.4	248	8.13	18.7	66.6

Table 2
Monthly operation of the CSP plant (Martín and Martín, 2013).

	January	February	March	April	May	June	July	August	September	October	November	December
Q**(kW)**	18,650	21,610	22,460	27,120	28,400	36,450	36,870	30,940	25,850	17,380	14,830	13,990
$T_{in,\ air}$**(°C)**	12.5	13.2	14.7	16.4	19.1	22.7	25.7	26.4	24.0	20.0	16.2	13.7
T_v **(°C)**	59.7	59.7	59.7	59.7	59.7	59.7	59.7	59.7	59.7	59.7	59.7	59.7
P_{gen}**(kW)**	12,623	14,632	15,206	18,362	19,222	24,673	24,959	20,943	17,201	11,763	10,042	9468

$$f^i(m) \cdot b_{fan}(m) \geq n_b^i(m) \tag{22}$$

$$n_{fan}(m) = \sum_{i=1}^{n_{fan}} f^i(m) \tag{23}$$

Variable b_{fan} is defined considering that, after the design of the equipment, the pipes bundles will be distributed equitably among the fans.

–Power's equation: the Eqs. (24) and (25):

$$P_{vent}(m) = \sum_{i=1}^{n_{fan}} P_F^i(m) \tag{24}$$

$$\begin{aligned}\Delta p_e^i(m) \;=\; & \Delta p_{Fs}^i(m) + 4.5922 \times 10^{-8} \cdot \left(m_{fan}^i(m)\right)^2 \\ & + 4.5922 \times 10^{-8} \cdot \left(m_{fan}^i(m)\right)^2 + 9.38925 \times 10^{-6} \cdot \left(m_{fan}^i(m)\right)^2 \\ & + 1.1207 \times 10^{-5} \cdot \left(m_{fan}^i(m)\right)^2 + \left(-6.2129 \times 10^{-8} \cdot V_{air}^i(m)\right. \\ & \left. + 1.3642 \times 10^{-4}\right) \cdot \left(m_{fan}^i(m)\right)^2 \\ P_{vent}(m) \;=\; & \sum_{i=1}^{n_{fan}} \left(\Delta p_e^i(m) \cdot m_{fan}^i(m)\right)\end{aligned} \tag{25}$$

–Redefined equations: the Eqs. (26) and (27) are defined using the variable n_b in order to calculate $A_{in}(m)$and $A_{out}(m)$:

$$A_{in}(m) = n_b^{tot}(m) \cdot N_t \cdot N_r \cdot A_{in,pipe} \tag{26}$$

$$A_{out}(m) = n_b^{tot}(m) \cdot N_t \cdot N_r \cdot A_{out,pipe} \tag{27}$$

–The objective function is given by Eq. (28) aiming at the minimum annual consumption of energy. We consider a base of 20 kW as the power required to switch on a fan:

$$Z = n_{cycles}\left(\sum_{m=1}^{12}\sum_{i=1}^{n_{fan}}\left(P_F^i(m) + 2000 \cdot f^i(m)\right)\right) + n_{cleaning} \cdot C_{cleaning} \tag{28}$$

The problem size depends on the years of continuous operation up to 6350 equations, 5800 continue and 1440 discrete variables. We use a commercial MINLP solver DICOPT, but if no integer solutions are reported, an approximation method is used instead by using the continuous solution provided and rounding the continuous solutions up. Alternatively, a rolling horizon kind of scheme can be implemented.

4. Results

We use as a case study the Concentrated Solar Power facility developed in Martín and Martín (2013) based on an actual facility in Spain. It is a small facility producing around 20 MW a year, located in a region where solar incidence is high and the availability of water is becoming a challenge. Results section is divided into three subsections. In Section 4.1 we present the cooling needs of the CSP plant and the monthly atmospheric data. Section 4.2 discusses the main design features of the unit. Finally, Section 4.3 presents the operation and optimal cleaning instances.

4.1. Operating data

The facility is located in the same region as the one in the work by Martín and Martín (2013). The operating conditions, weather data and plant operation are collected and summarized in Tables 1 and 2. We assume that over the time horizon the average monthly conditions are the same every year. Further studies on the effect of uncertainty are out of the scope of this work.

4.2. Equipment design

A Branch and Bound method was applied for the design of units for different years of operation before the removal of the deposits. The solution of each design takes about 30 min of CPU time in an Intel i5 core running under Windows 10. Based on a life span of the unit of 16 years, the number of maintenance shutdowns determines the length of the cycle. We consider at least one and a maximum of 3 shutdowns since for 3 years fouling does not show performance decays and a minimum cycle of 4 years is considered. Table 3 shows the designs resulting for 4, 5, 6, 8 and 12 years of operation for 1 to 3 maintenance shutdowns. We can see that most of the characteristics are the same. The fan blades angles are within 16° and 16.5°. The general trend is that the blade angle

Table 3
Major design characteristics of the A frame design for different years of continuous operation.

Variable	Years of operation				
	12	8	6	5	4
Air flow (kg/s)	2641.83	2641.83	2641.83	2641.83	2641.83
T out (K)	313.00	313.00	313.00	313.00	313.00
Apex. (°)	64.15	63.89	63.87	63.82	64.30
L (m)	15.00	15.00	15.00	15.00	15.00
Dext (m)	0.033	0.033	0.033	0.033	0.034
Dint (m)	0.027	0.027	0.027	0.027	0.028
Nt	75	75	75	75	75
Nr	1	1	1	1	1
nb	16	16	16	16	16
Df (m)	0.053	0.053	0.056	0.061	0.044
nf	64.918	58.963	39.957	19.62	10
Number of fines per tube	974	884	599	294	150
pitch_t (m)	0.15	0.15	0.15	0.15	0.15
pitch_l (m)	0.15	0.15	0.15	0.15	0.15
n_fans	4	4	4	4	4
Beta (°)	16.54	16.52	16.38	16.24	16.14
Qfan (m^3/s)	557.82	557.82	557.82	557.82	557.82
L_ts (m)	6.00	6.00	6.00	6.00	11.12
d_ts (m)	0.10	0.10	0.10	0.10	0.10
x_up (m)	0.60	0.60	0.60	0.60	0.60
x_do (m)	1.50	1.50	1.50	1.50	1.50
Aext (m^2)	5095.777	4889.542	4220.582	3376.233	2191.516
Coste vent ($)	1,651,970	1,651,820	1,651,090	1,650,340	1,649,770
MenVent ($/month)	7648	7647	7644	7640	7638
Cost ($)	91,401	89,917	84,827	77,649	65,433
MenAframe ($/mes)	305	300	283	259	218
Cost ener ($/month)	78,190	78,071	77,487	76,897	76,446
Power (W)	9.46E+5	9.44E+05	9.37E+05	9.30E+05	9.25E+05
Z ($/month)	**86,142.60**	**86,018.20**	**85,414.10**	**84,796.00**	**84,302.00**

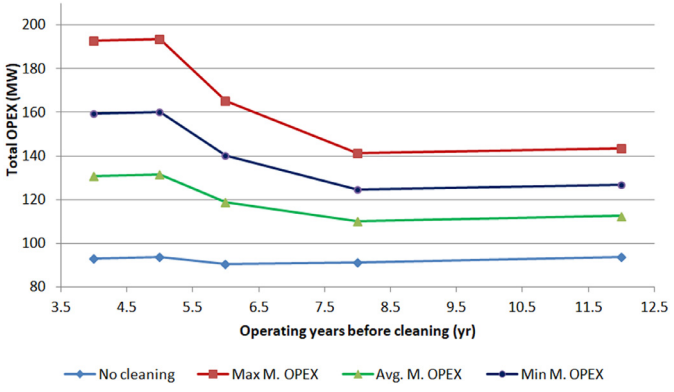

Fig. 4. Operating cost over time under fouling conditions.

slightly increases with the length of the operating cycle. Small differences can also be seen in the angle of the A-frame, from 63.8° to 64.3°, which can be due to numerical issues. Most of the units are designed with an apex of 60°, a result that has already been obtained in the literature (Conradie et al.,1998). Furthermore, the bundle of pipes consists of a single line of 75 pipes in all cases. The number of tubes per row is larger compared to typical designs in the literature, around 60 (Pieve and Salvadori, 2011) or 56 for the horizontal design (Manassaldi, 2014). Note that those studies do not consider fouling. A total number of 8 two-side bundles is to be installed to reject the heat during the month of the largest power production capacity, July. The diameter of the pipes is the same in all cases as well as its length, 15 m. However, in the literature shorter tubes are typically installed, 9 m (Kröger, 2004) or 10.9 m (Manassaldi, 2014). The only major difference between the designs for the different operating cycle lengths is given by the tube fines. It increases with the number of years of continuous operation. This can be due to the fact that the longer the operation period the lower the heat transfer coefficients due to the fouling resistance, and larger heat transfer areas are required. As a result of the larger number of fines, the area available increases from 2000 m^2 to 5000 m^2 when the operating period reaches 12 years. The size of the fines also changes with the operating period before cleaning, but there is no clear trend, mostly due to the large number of degrees of freedom. In the literature, the typical number of fines is around 393.7 fines per m (Manassaldi, 2014). The difference between this value and our results is due to the lack of constraints on the projected area of the unit. Aiming at lower pressure drop results in a design that increases the open area in the pipe layout.

The comparison between the design under no fouling conditions (Luceño and Martín, 2018) with the results in this work is not a fair one. However, it is interesting to see the changes in the geometric characteristics as a result of fouling. The length of the pipes is larger when fouling is considered, from 13.5 m in case of a clean design to 15 m in case of considering fouling. The number of fines selected for the clean operation corresponds to a value in between those corresponding to 5 and 6 years of operation under fouling conditions, and the apex angle is a little smaller, around 62°. Finally the pitch distances are larger than the one in other designs (Manassaldi, 2014; Conradie et al., 1998), to reduce the pressure drop. In general, larger areas will be required when fouling is considered and therefore the changes in the designs are related to that.

4.3. Operation

For the optimal geometry of the unit obtained for each cycle time, we optimize the operation of the system for minimum power consumption. Therefore, the problem becomes a multiperiod MINLP optimization problem. The multiperiod problem for each cycle time takes from 25 min to 30 min depending on its length in an Intel i5 computer running under Windows 10. Thus,

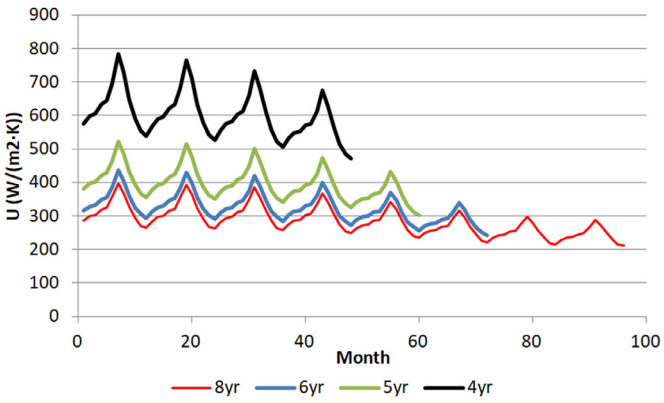

Fig. 5. Profile of the global heat transfer coefficient under fouling conditions.

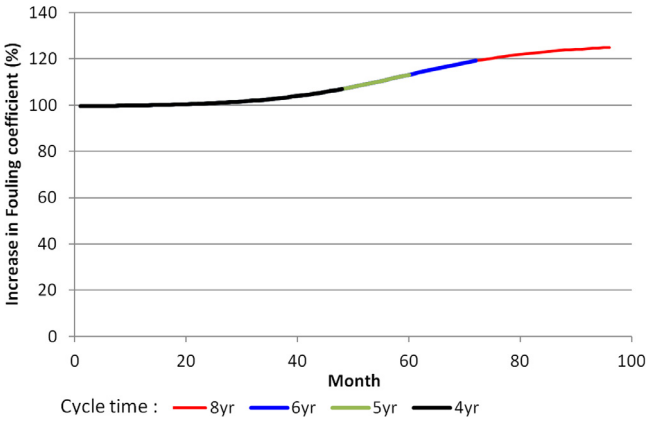

Fig. 6. Profile of the fouling coefficient.

it is up to the operation to decide the number of fans used, the outlet air temperature and the flow used per fan. We assume that for a fan to operate, a minimum flow rate of 50 m^3/s is required. 4 and 5 years cycle length can be solved to integral solutions, but longer cycles needed for the continuum solution to be rounded up. We also tried BARON, but reducing the optimality gap below 10% was rather difficult and the solutions obtained were similar to the approximated ones. It is out of the scope of this work to pursue a more accurate solution method. However, it will be an interesting future work.

Fig. 4 shows the results of the comparison of the operation over 4, 5, 6, 8 and 12 years. When no cleaning costs are considered, or if cleaning can be performed during non-operating periods when solar is not included in the energy mix, there is an optimum value of 6 years of operation before cleaning. Beyond 6 years the operating cost increases slightly. However, the cost savings when operating in 6 years cycles compared to operating for 8 years are small. Over 8 years the operation cost slightly increases. Next, the cleaning costs are assumed to be between the energy not produced in January, the month with the lowest power production, and July, the month of the largest power produced. Furthermore a third value, the average production of the facility over a year is assumed too, see Table 2 for the actual values. Note that this does not mean that the plant will stop for an entire month for cleaning. When different costs for cleaning are added, it turns out that longer operating periods are favored. However, for 12 years of operation before cleaning the operating costs increase with or without considering cleaning costs. Thus, we consider that the optimal cycle time is 8 years. The particular fouling building-up profile results in the fact that there are small additional losses of efficiency over 8 years while the number of shutdowns is just one instead of 2 in case 6 years is selected as cycle time and therefore, the operating cycle of 8 years is preferred. However, if a different profile is found, the results may be affected and shorter or longer cycle times would be

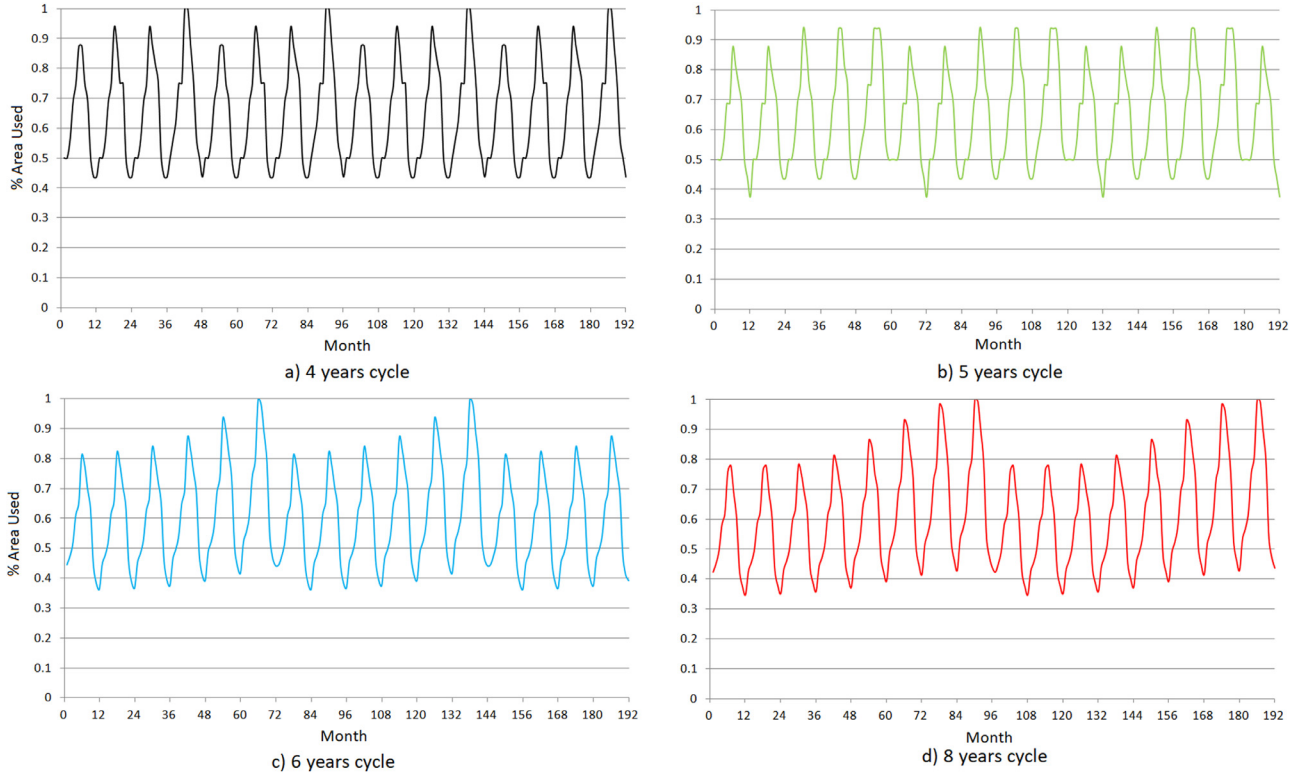

Fig. 7. Fraction of area used over time.

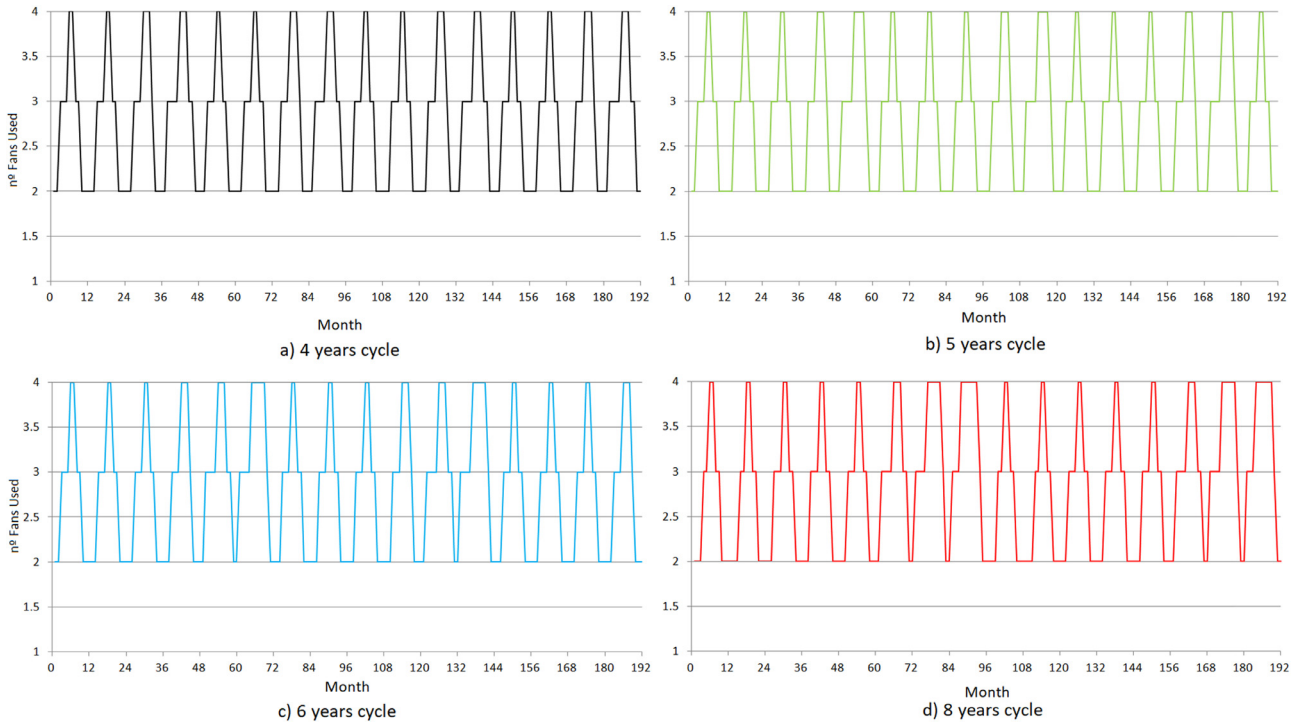

Fig. 8. Number of fans of operation over time.

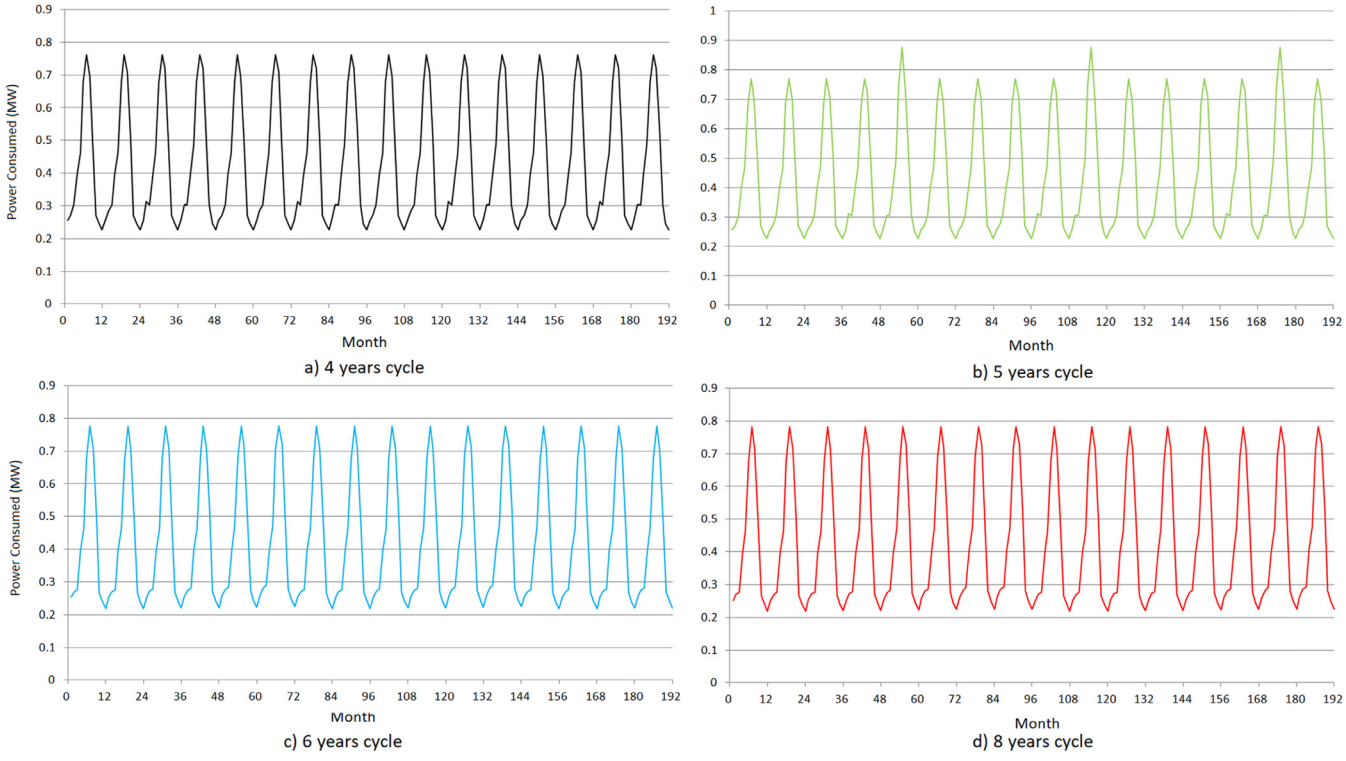

Fig. 9. Power consumption over time.

selected since a minimum would have been found in the parametric optimization approach.

Next, we present the results of the operation for cycle lengths of 4, 5, 6 and 8 years. Fig. 5 shows the profile of the global heat transfer coefficient over time. The shorter the cycle, the larger the U. The global heat transfer coefficients are larger for cleaner pipes since deposits have not had the time to build-up. To provide additional transfer area to mitigate the smaller U's when the operating cycle is longer, a larger number of fines are required. If we operate for 8 years, the number of fines is around six times the ones suggested for an operating cycle of 4 years. Fig. 6 shows the increase in the pressure drop due to fouling over time. Note that this increment only affects one of the terms of Eq. (10), and that at most this term only increases up to 25% by the end of the operating cy-

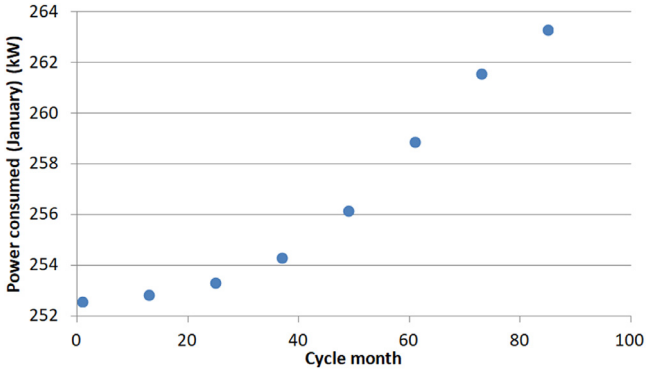

Fig. 10. Increase in power consumption over time for a cycle. 8 years of cleaning cycle.

cle. The plateau reached by the pressure drop results in the fact that longer operating times are reasonable to operate. A different profile, linear for instance, would have changed the decision over the operating cycle time since a clear minimum is expected to have appeared.

The operating results for the different cycle lengths considered including the effect of fouling on the heat transfer resistance and the pressure drop are presented in Figs. 7–12. Fig. 7 shows the fraction of area used for all four cycle lengths. The area required increases over time. The shorter the cycle, the smaller the increase in the area needed before cleaning. A merely 10% additional area is needed if we operate in a 4 year cycle, but it goes over 20% increase for the optimal case of 8 years of continuum operation. The cycle length is identified easily. By the end of the cycle the maximum area is used, typically almost the entire area available by design. Furthermore, after cleaning, the area usage is reduced again. Only in the case of 5 years the available area is not fully used.

Fig. 8 shows the number of fans in operation over time. We see that as the cycle time before cleaning increases, the usage of the fans increases too. Over summer time, it is necessary to use 3 and 4 fans over longer periods of time due to the increase in the pressure drop and the need to move a larger air flow rate. Just before cleaning the fans capacity is fully used, the peaks of use are wider in Fig. 8. This poses a high stress on the fan system. However, the fans are a more efficiently used for larger operating cycles, otherwise, a large section of the unit remains idle for longer periods of time. Idle units are a burden for the economy of these facilities.

Fig. 9 shows the power production over time. It is not easy to see that the longer the cycle the higher the power consumed due to fouling resistance to the air flow. The reason is the relatively small increase in power consumption due to fouling. To present that effect more clearly, for the optimal solution, 8 years of operation, Fig. 10 compares the power consumed every January over the entire cycle. It shows the effect of building up in the pressure drop and the increase in the power consumed. The increase follows the sigmoid that represents the increase in pressure drop due to fouling.

For the sake of the length of the work we only present the flow rates per fan for the optimal case, an operating cycle of 8 years. Based on the assumption that every year the plant operation is the same, the air flow rate across the system for any particular month is the same over the horizon studied. The particular power curves of the fans suggest the use of a second fan even before the first one reaches it full capacity. In spite of the increase in the pressure drop, typically the operation of the fan is symmetric over time. We cannot ascertain that the differences are not related to numerical

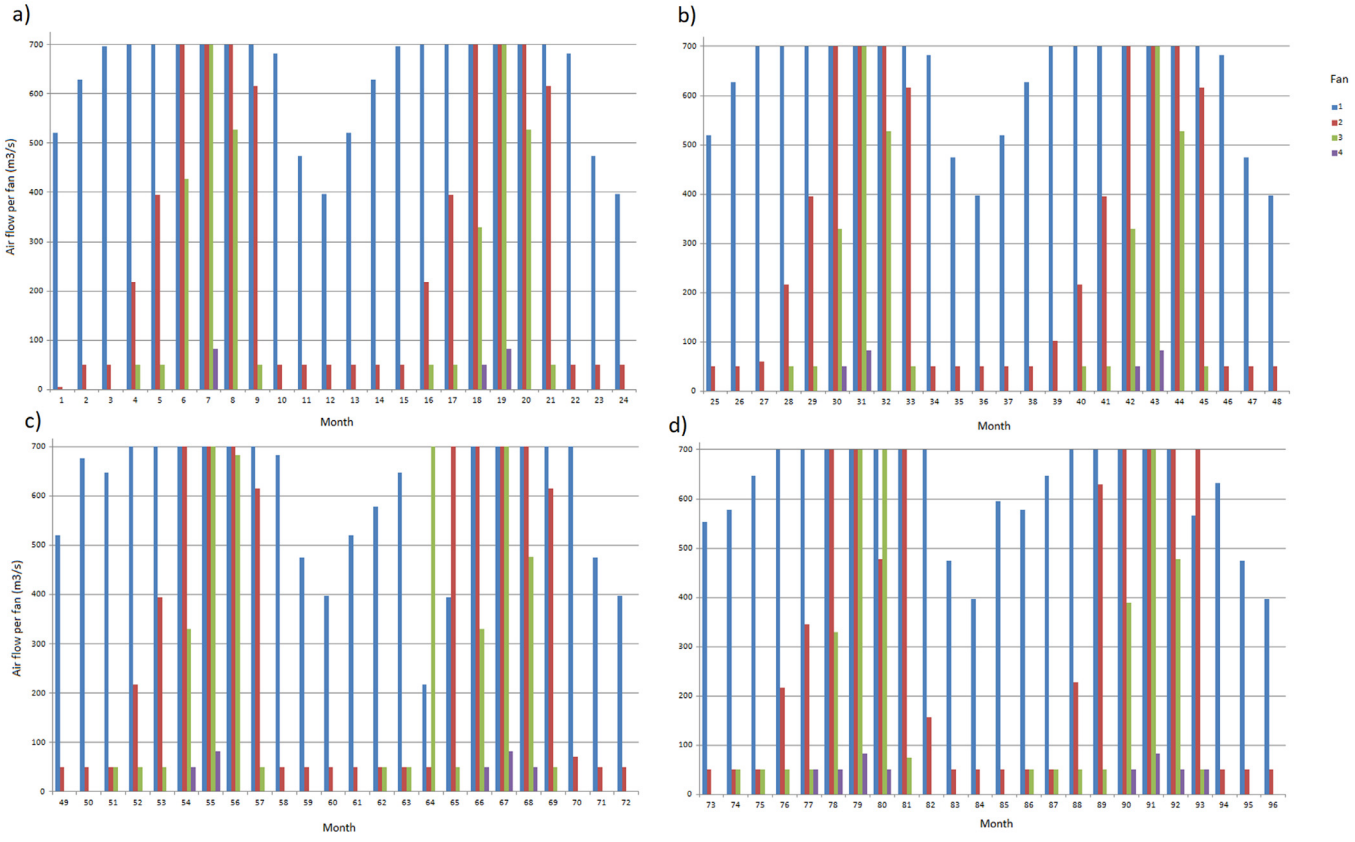

Fig. 11. Air flow across each of the operating fans. 8 years cycle. (a) 0–2 years; (b) 2–4 years; (c) 4–6 years; (d) 6–8 years.

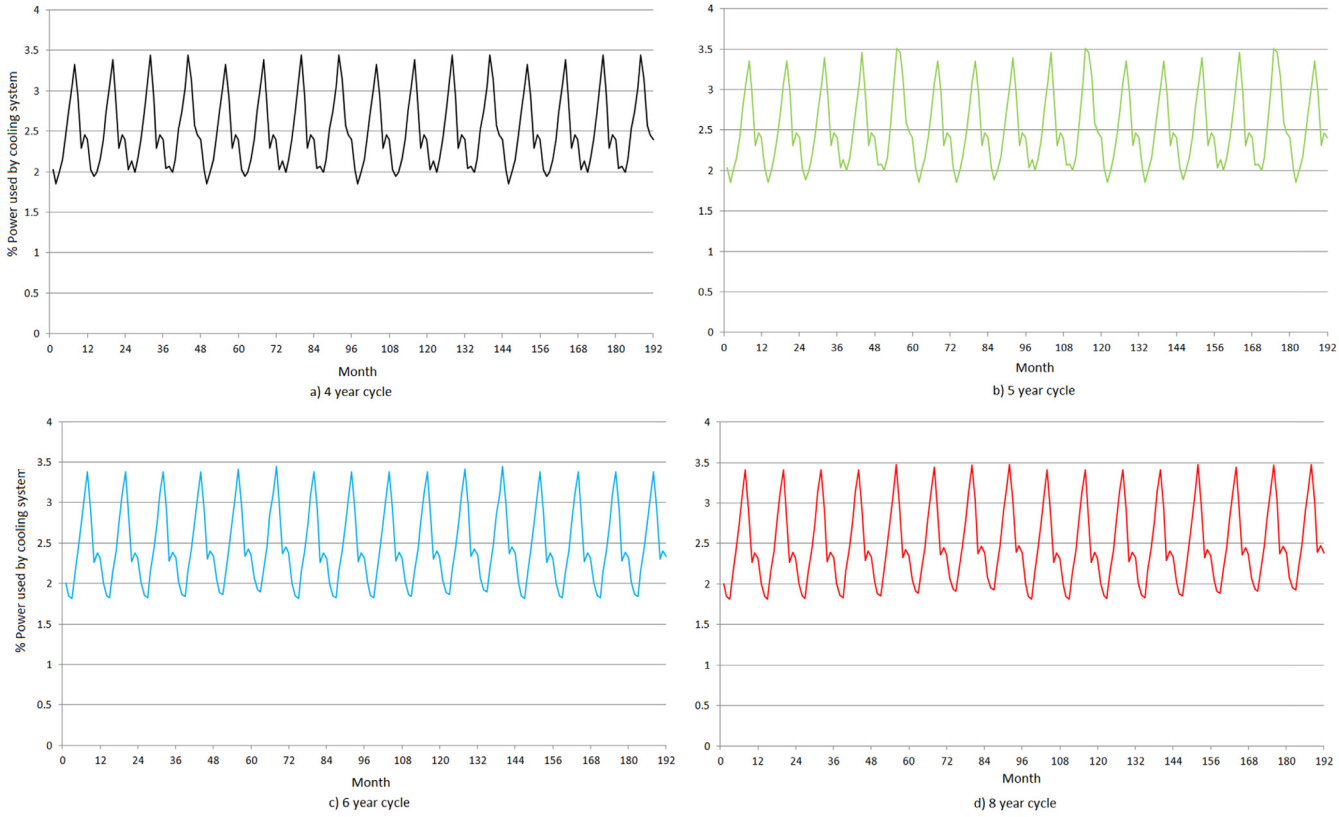

Fig. 12. Fraction of power used by fans.

issues, see Fig. 11. Four subplots are show (a)–(d) to present a 2 year period for plot for clarity.

Finally, Fig. 12 shows the percentage of the produced energy used over time to power the fans. A maximum of 3.5% is found using summer periods, but the range is from 2% in winter to 3.5% in July. We see that the power consumed fraction increases slightly over time between cleaning stages, but the increase is not large since, as we saw in Fig. 9, the total power consumption only increases slightly due to fouling.

The operation of solar based facilities shows high dependency with the weather conditions on both the energy source and the cooling devices. So far deterministic designs have been evaluated (Luceño and Martín, 2018) and this work. However, the operation of the system must include solar incidence variability and weather conditions. Future work will focus on addressing uncertainty in the design of air cooling systems and its integration with CSP facilities.

5. Conclusions

In this work we have presented a parametric optimization framework for the optimal design and operation of units subjected to performance decays over time. We have applied it to the design of A-frame dry cooling systems under fouling conditions. The model for the A-frame is detailed following the typical design of heat exchangers including pipes layout and size and fans performance. The particular feature is the addition of a model to evaluate the effect of particle deposition on the pipes of the A-frame on both the pressure drop and the resistance to the heat transfer. A two-stage procedure is proposed for the optimal design, and unit operation to evaluate the operating time before cleaning. The unit is designed by solving an MINLP problem including the geometry of the A-frame for the month of the largest cooling load between 3 and half the unit life. We compute the monthly U for that configuration in the last year of operation and with that as reference, the U for each month of the operating cycle. In a second step, we optimized the monthly operation of the unit by formulating a multi-period MINLP for the various cycle lengths. Cleaning costs are added in terms of power not produced. The solution of this problem indicates not only the optimal cleaning schedule, but also the use of the number of fans, the air flowrate and its inlet and outlet temperature.

The solution suggested an operating cycle of 8 years for the case of a sigmoid profile for dust deposition. The units main characteristics are an apex angle of 63.8°, one row of 75 pipes of 15 m long and with a diameter of 3.3 mm. A total of 4 fans are used but they only operate at full capacity during summer. The number of fans in operation increases for the central months of the years by the end of the cycle time. The optimization allows a reduced power usage to operate the fans, always below 4%, even though this value increases over the operating cycle before the next cleaning stage. For larger cycle lengths the solution is to be approximated from the continuous one due to the size of the model. A more accurate problem reformulation can help solve the problem such as the use of a rolling horizon framework.

Acknowledgements

The authors would like to acknowledge Salamanca Research for optimization software licenses. The authors acknowledge the TCUE fellowship from Fundación Universidad – Empresa USAL 2015 to Mr. JA Luceño.

Supplementary materials

Supplementary material associated with this article can be found, in the online version, at doi:10.1016/j.compchemeng.2018.05.015.

References

Ahn, Y., Cheong, S., Jung, Y., Lee, J., 2006. An experimental study of the air-side particulate fouling in fin-and-tube heat exchangers of air conditioners. International Refrigeration and Air Conditioning Conference. Paper 818 http://docs.lib.purdue.edu/iracc/818.

Al-Haj Ibrahim, H., 2012 Fouling in Heat Exchangers. MATLAB – A Fundamental Tool for Scientific Computing and Engineering Applications – Volume 3 dx.doi.org/10.5772/46462.

Beaurepaire, P., Valdebenito, M.A., Schueller, G., Jensen, H.A., 2012. Reliability –based optimization of maintenance scheduling of mechanical components under fatigue. Compt. Methods. Appl. Mech Eng. 1 (221–222), 24–40.

Bell, IH., Groll, E.A., Koning, H., Odrich, T., 2009. Experimental analysis of the effects of particulate fouling on heat exchanger heat transfer and air side pressure drop for a hybrid dry cooler. In: Proc. Int. Conf. Heat Exchanger Fouling and Cleaning. 2009. Austria.

Bredell, J.R., Kröger, D.G., 2006. Numerical Investigation of Fan Performance in a Forced Draft Air-Cooled Steam Condenser. California Energy Commission, California.

Chen, J.J., 1987. Letter to the editor: Comments on improvement on a replacement for the logarithmic mean. Chem. Eng. Sci. 42, 2488–2489.

Coker, A.K., 2007. Ludwig's Applied Process Design for Chemical and Petrochemical Plants, 4th ed. Elsevier, Oxford.

Conradie, A.E., Buys, J.D., Kroger, D.G., 1998. Performance optimization of dry-cooling systems for power plants through sqp methods. Appl. Therm. Eng. 18 (1–2), 25–45.

Damaso, V.C., García, P.A.A., 2009. Testing and preventive maintenance scheduling optimization for aging systems modeled by generalized renewal process. Pesquisa Oper. 29 (3), 563–576.

Dekker, R., 1996. Application of maintenance optimization models: a review and analysis. Rel. Eng. Sys. Saf. 51, 229–240.

Díaz-Bejarano, E., Coletti, F., Macchietto, S., 2017. Thermo-hydraulic analysis of refinery heat exchangers undergoing fouling. AIChE J. 63 (3), 984–1001.

DOE Last accessed January 2018.

FAO [last accessed February 2018].

GEA 2008 Industrial air-cooled heat exchangers, and the effects of air side fouling 207-211

Haghighi-Khoshkhoo, R., McCluskey, F.M.J., 2007. Air-side fouling of compact heat exchangers for discrete particle size ranges. Heat Transf. Eng. 28 (1), 58–64.

Heyns, J.A., 2008. Performance Characteristics of an Air-Cooled Steam Condenser Incorporating a Hybrid (Dry/Wet) Dephlegmator M.Sc. Thesis. University of Stellenbosch, Stellenbosch, South Africa.

Kern, D.Q., Seaton, R.E., 1959. A theoretical analysis of thermal surface fouling. Br. Chem. Eng. 4 (5), 258–262.

Kijima, M., Sumita, N., 1986. A useful generalization of renewal theory: counting process governed by non-negative Markovian increments. J. Appl. Probab. 23, 71–88.

Kröger, D.G., 2004. Air-Cooled Heat Exchangers and Cooling Towers: Thermal-Flow Performance Evaluation and Design, II. Pennwell, Oklahoma, Tulsa.

Liu, L.L., Fan, J., Chen, P.P., DU, J., Yang, F-L., 2015. Synthesis of heat exchanger networks considering fouling, ageing and cleaning. Ind. Eng. Chem. Des 54 (1), 296–306.

Luceño, J.A., Martín, M., 2018. Optimal design and operation of A-frame systems for solar power plants. in press. Energy.

Luo, X., Xia, C., Sun, L., 2013. Margin design, online optimization, and control approach to heat exchanger network with bypasses. Comp. Chem. Eng. 53, 102–121.

Manassaldi, J.I., Scenna, N.J., Mussati, S.F., 2014. Optimization mathematical model for the detailed design of air cooled heat exchangers. Energy 64, 734–746.

Martín, M., 2015. Optimal annual operation of the dry cooling system of a concentrated solar energy in the South of Spain. Energy 84, 774–782.

Martín, L., Martín, M., 2013. Optimal year-round operation of a concentrated solar energy plant in the South of Europe. App. Therm. Eng. 59, 627–633.

Martin, M., Martín, M., 2017. Cooling limitations in power plants: optimal multi-period design of natural draft cooling towers. Energy 135, 625–636.

Matche [last accessed February 2018].

MPR, 2014. Ministerio de la Presidencia. Ley 24/2014, de 24 de noviembre, del Impuesto sobre Sociedades. Boletín Oficial del Estado 288, 96939–97097 [last accessed February 2016].

Mukerji, R., Merrill, H.M., Erickson, B.W., Parker, J.H., Friedman, R.E., 1991. Power plant maintenance scheduling: optimizing economics and reliability. IEEE Trans. Power Syst. 6 (2), 476–483.

Muller-Steinhagen, H, Reif, F, Epstein, N, Watkinson, AP, 1988. Influence of operating conditions on particulate fouling. Can. J. Chem. Eng. 66, 42–50.

Muller-Steinhagen, H., Malayeri, M.R., Watkinson, A.P., 2005. Fouling of heat exchanger-new approaches to solve old problem. Heat Transf. Eng. 26 (2), 1–4.

Müller-Steinhagen, H., Malayeri, M.R., Watkinson, P., 2011. Heat exchanger fouling: mitigation and cleaning strategies. Heat Trans. Eng. 32 (3–4), 189–196.

MPR, Ministerio de la Presidencia, 2014. Ley 24/2014, de 24 de noviembre, del Impuesto sobre Sociedades. Boletín Oficial del Estado 288, 96939–97097 [last accessed February 2016].

Nguyen, D.Q., Brammer, C., Bagajewicz, M., 2008. New tool for the evaluation of the scheduling of preventive maintenance for chemical process plants. Ind. Eng. Chem Res. 47 (6), 1910–1924.

Pak, B.C., Baek, B.J., Groll, E.A., 2003. Impacts of fouling and cleaning on the performance of plate fin and spine fin heat exchangers. KSME Int. J. 17 (11), 1801–1811.

Pieve, M., Salvadori, G., 2011. Performance of an air-cooled steam condenser for a waste-to-energy plant over its whole operating range. Energy Conv. Manag. 52, 1908–1913.

Pu, H., Ding, G.-l., Ma, X.-K., Hu, H.-T., Gao, Y.F., 2009. Effects of biofouling on air–side heat transfer and pressure drop for finned tube heat exchangers. Int. J. Refrig. 32 (5), 1032–1040.

Rosegrant, M.W., Cai, X., Cline, S.A., 2002. Global Water Outlook to 2025: Averting an Impending Crisis. International Food Policy Research Institute, Washington, DC.

Sarfraz, O., Bach, C., 2016. A literature review on heat exchanger air side fouling in heating, ventilation and air conditioning (HVAC) applications. International Refrigeration and Air Conditioning Conference. Paper 1663.

Tan, J.S., Kramer, M.A., 1997. A general framework for preventive maintenance optimization in chemical process operations. Comput. Chem. Eng. 21 (12), 1451–1469.

The Engineering Toolbox [last accessed February 2018].

Towler, G., Sinnott, R., 2008. Chemical Engineering Design. Elsevier, Oxford. UK.

Walas, S.M., 1990. Chemical Process Equipment: Selection and Design. Butterworth-Heinemann, Boston. USA.

Wang, H., 2002. A survey of maintenance policies of deteriorating systems. Eur. J. Oper. Res. 139 (3), 469–489.

Yang, L., Braun, J.E., Groll, E.A., 2007. The impact of evaporator fouling and filtration on the performance of packaged air conditioners. Int. J. Refrig. 30 (3), 506–514.

Zammit, K., 2005. Air-Cooled Condenser Design, Specification, and Operation Guidelines. Electric Power Research Institute, California, Palo Alto.